

# Gamma-Jet Tomography of Quark-Gluon Plasma in High-Energy Nuclear Collisions

Hanzhong Zhang<sup>a,b</sup> J. F. Owens<sup>c</sup> Enke Wang<sup>a,b</sup> and Xin-Nian Wang<sup>d</sup>

<sup>a</sup>*Institute of Particle Physics, Huazhong Normal University, Wuhan 430079, China*

<sup>b</sup>*Key Laboratory of Quark and Lepton Physics (Huazhong Normal University), Ministry of Education, China*

<sup>c</sup>*Physics Department, Florida State University, Tallahassee, Florida 32306-4350, USA*

<sup>d</sup>*Nuclear Science Division, Lawrence Berkeley Laboratory, Berkeley, California 94720, USA*

---

## Abstract

Within the next-to-leading order (NLO) perturbative QCD (pQCD) parton model, suppression of away-side hadron spectra associated with a high  $p_T$  photon due to parton energy loss is shown to provide a complete tomographic picture of the dense matter formed in high-energy heavy-ion collisions at RHIC. Dictated by the shape of the  $\gamma$ -triggered jet spectrum in NLO pQCD, hadron spectra at large  $z_T = p_T^h/p_T^\gamma \gtrsim 1$  are more susceptible to parton energy loss and therefore are dominated by surface emission of  $\gamma$ -triggered jets, whereas small  $z_T$  hadrons mainly come from fragmentation of jets with reduced energy from volume emission. These lead to different centrality dependence of the hadron suppression in different regions of  $z_T$ .

---

Jet quenching [1] has become a powerful tool for the study of the quark-gluon plasma [2] in high-energy nuclear collisions. Jets are produced in the early stage of heavy-ion collisions through hard parton scattering. When they pass through the dense matter, they will interact with the medium and lose a significant amount of their energy via gluon radiation induced by multiple scattering.

In our previous studies based on a NLO pQCD parton model [3, 4], we checked the tomographic pictures of single jets and di-jets by a simultaneous fit to single hadron and dihadron data. Single hadrons are dominated by the jet emissions close and perpendicular to the surface of the system, while dihadrons are emitted both close and tangential to the surface of the system although there are contributions from punch-through jets from the central region. However, the dominance of surface and tangential emission makes it difficult to extract the space-time profile of the dense medium from single and dihadron spectra.

Here we focus on the study of photon-triggered away-side hadron spectra coming from  $\gamma$ -jet events in central nucleus-nucleus collisions [5]. By selecting  $\gamma$ -hadron pairs with different values of  $z_T = p_T^h/p_T^\gamma$  which could be larger than 1 due to radiative correction in NLO pQCD, one can effectively control hadron emission from different regions of the dense medium and therefore extract the corresponding jet quenching parameters. For the study of photon-hadron correlation in this paper, we focus mainly on photon production with isolation cuts [5, 6]. Therefore, we can neglect those photons that are produced via induced bremsstrahlung [7], jet-photon conversion [8] and thermal production [9, 10] in high-energy heavy-ion collisions.

Within the same energy loss formalism as in our previous studies on single and dihadron [4], we calculate the production of the photon-triggered hadron spectrum in central Au+Au collisions at  $\sqrt{s} = 200$  GeV. Shown in Figure 1 are our numerical results for  $D_{pp}(z_T)$  or  $D_{AA}(z_T)$

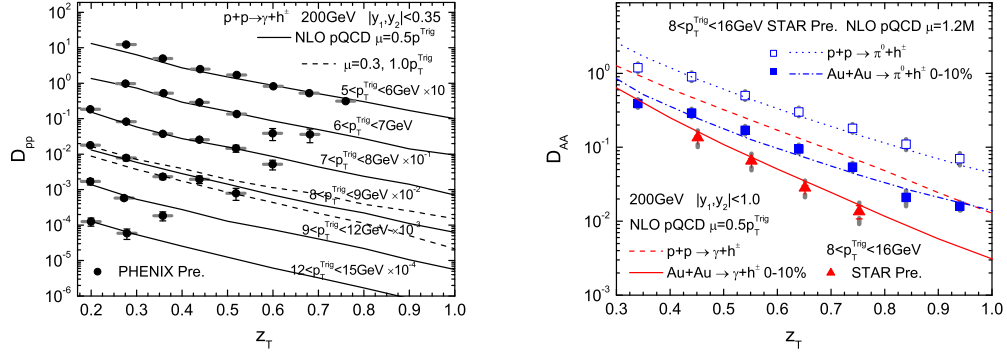


Figure 1:  $\gamma$ -triggered and hadron-triggered FF's in p+p and central Au+Au collisions at the RHIC energy. The preliminary data are from [11, 12]. Systematic errors of experimental data are shown as shaded bars when available.

[5] compared to data. The left plot is for gamma-hadron spectra in p+p collisions. They fit the PHENIX preliminary data very well for different values of  $p_T^{trig}$ . We also show the uncertainties (dashed curves) due to the choice of the factorization scale, which mainly comes from the scale dependence of the FF's. In the right plot we show the gamma-hadron spectra in central Au+Au collisions (solid curve) as compared to p+p collisions (red dashed curve). The NLO pQCD prediction for the suppression of gamma-hadron spectra agrees well with the STAR preliminary data. Such an agreement is extremely nontrivial given the completely different emission geometry as compared to single and dihadron productions as we will see below, and it reinforces the success of the parton energy loss picture for the observed jet quenching phenomena. Also shown in the right plot are the calculated hadron-triggered FF's, the dotted curve for p+p collisions and the dot-dashed curve for central Au+Au collisions, as compared to the experimental data. Hadron-triggered FF's are larger than photon-triggered FF's for both p+p and A+A collisions mainly because the fraction of hadron-triggered gluon jets is larger than the fraction of photon-triggered gluon jets at same  $p_T^{trig}$ , and the hadron yield of gluon jets is larger than that of quarks.

The nuclear modification factor  $I_{AA}$  for the photon-triggered hadrons  $I_{AA} = D_{AA}/D_{pp}$  is defined to characterize the effect of jet quenching. Shown in the left plot of Figure 2 are the calculated nuclear modification factors both in LO (dot-dashed) and NLO (solid) calculations of gamma-triggered FF's. In the LO pQCD calculation, transverse momentum of the associated jet is balanced exactly by the direct photon in tree  $2 \rightarrow 2$  processes. This limits  $z_T = p_T^h/p_T^\gamma \leq 1$ . In the NLO, however, radiative correction permits  $z_T > 1$  for gamma-hadron productions. The two effects give rise to NLO  $I_{AA}$  very different from LO results. Therefore, to exactly probe the dense matter from gamma-hadron correlations, one must use NLO pQCD calculations. .

Also shown in the left plot of Figure 2 is the dihadron suppression factor, dashed curve. Compared with dihadron  $I_{AA}$ , gamma-hadron  $I_{AA}$  has a more stronger dependence on  $z_T$ . One can imagine that the gamma-triggered jets contributing to large- $z_T$  gamma-hadron are more susceptible to energy loss. Even a small amount energy loss can greatly suppress the large- $z_T$  gamma-hadron yield. So large- $z_T$  gamma-hadrons are dominated by those gamma-triggered jets originating near and escaping through the surface almost without energy loss. Similar to sin-

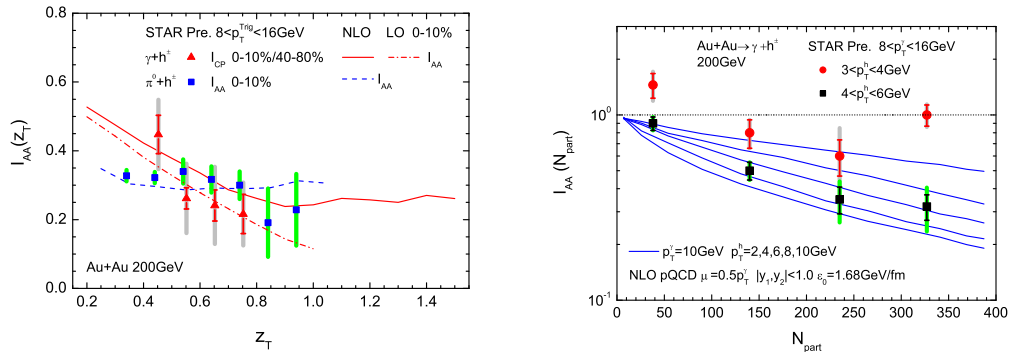


Figure 2: The nuclear modification factor  $I_{AA}$  for  $\gamma$ -triggered fragmentation function in central  $Au + Au$  collisions at the RHIC energy. The data are from [11]. In the left plot for  $I_{AA}(z_T)$  the triggered photon is chosen with  $p_T^\gamma = 8 - 16$  GeV. In the right plot for  $I_{AA}(N_{part})$  the triggered photon is chosen with  $p_T^\gamma = 10$  GeV and the associated hadron with  $p_T^h = 2, 4, 6, 8, 10$  GeV, respectively (from top to bottom).

gle hadron suppression factor, large- $z_T$   $I_{AA}$  is mainly determined by the thickness of the corona of the surface emission. The picture of the surface emission is demonstrated by the left plot of Figure 3. The plot is the spatial transverse distribution of the initial gamma-jet production vertexes that contribute to the final gamma-hadron pairs with given values of  $z_T$ . The associated jets are considered along the right direction, and the opposite direction is for the triggered photons. The color strength represents the gamma-hadron yield from the fragmentation of the gamma-triggered jets after parton energy loss. The inserted panels are projections of the contour plots onto y-axes, solid curve without energy loss, dashed curve with energy loss. As for small  $z_T$  region, it has contributions from energetic jets originated from inside the medium that have lost a finite amount of energy before fragmenting into hadrons. That's why these gamma-correlated hadrons come from volume emission, as shown in the right plot of Figure 3. For the intermediate- $z_T$  region, gamma-hadrons are determined by the competition of the two emission mechanisms.

The above picture of volume and surface emission for the  $\gamma$ -triggered fragmentation function in heavy-ion collisions will lead to different centrality dependence of the nuclear modification factor  $I_{AA}(z_T)$  in different regions of  $z_T$ . Shown in the right plot of Figure 2 are nuclear modification factors for  $\gamma$ -triggered hadron spectra as functions of the participant number in  $Au + Au$  collisions at the RHIC energy for different values of  $z_T$  as compared to the STAR preliminary data. For small values of  $z_T < 1$ , the  $\gamma$ -triggered hadron yield is dominated by volume emission and therefore the centrality dependence of the nuclear modification factor is stronger than that in the region  $z_T \geq 1$  where surface emission is the dominant production mechanism.

In summary, high  $p_T$  photon-hadron correlations are studied within the NLO pQCD parton model with modified parton fragmentation functions due to jet quenching in high energy  $A + A$  collisions. We demonstrated that the volume (surface) emission dominates the  $\gamma$ -triggered hadrons spectra at small  $z_T < 1$  (large  $z_T \geq 1$ ) due to the underlying jet spectra in the NLO pQCD. Therefore, one will be able to extract jet quenching parameters from different regions of the dense medium by measuring the nuclear modification factor of the  $\gamma$ -triggered fragmentation

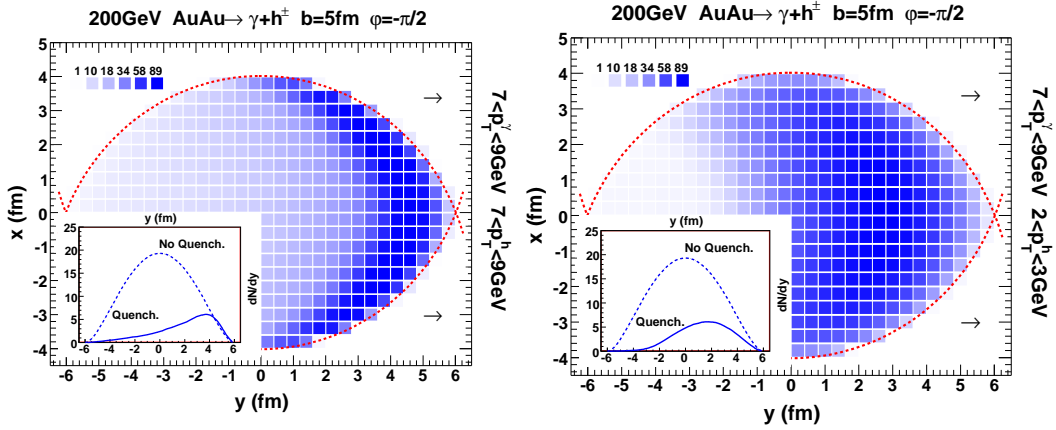


Figure 3: Transverse distributions of the initial  $\gamma$ -jet production vertices that contribute to the final observed  $\gamma$ -hadron pairs along a given direction (arrows) with  $z_T \approx 0.9$  (left plot) and  $z_T \approx 0.3$  (right plot).

function in the whole kinetic region, including  $z_T \geq 1$ , achieving a true tomographic study of the dense medium.

### Acknowledgements

This work was supported by DOE under contracts DE-AC02-05CH11231 and DEFG02-97IR40122, by NSFC of China under Projects No. 10825523 and No. 10875052 and No. 10635020, by MOE of China under Projects No. IRT0624; by MOST of China under Project No. 2008CB317106; and by MOE and SAFEA of China under Project No. PITDU-B08033.

### References

- [1] X. N. Wang and M. Gyulassy, Phys. Rev. Lett. **68**, 1480 (1992).
- [2] M. Gyulassy, I. Vitev, X. N. Wang and B. W. Zhang, arXiv:nucl-th/0302077; A. Kovner and U. A. Wiedemann, arXiv:hep-ph/0304151, in Quark Gluon Plasma 3, eds. R. C. Hwa and X.N. Wang, World Scientific, Singapore, 2003.
- [3] J. F. Owens, Rev. Mod. Phys. **59**, (1987)465.
- [4] H. Z. Zhang, J. F. Owens, E. Wang and X. N. Wang, Phys. Rev. Lett. **98**, 212301 (2007).
- [5] H. Z. Zhang, J. F. Owens, E. Wang and X. N. Wang, Phys. Rev. Lett. **103**, 032302 (2009).
- [6] H. Baer, J. Ohnemus, and J. F. Owens, Phys. Rev. D **42**, 61 (1990).
- [7] I. Vitev and B. W. Zhang, Phys. Lett. B **669**, 337 (2008).
- [8] R. J. Fries, B. Miller and D. K. Srivastava, Phys. Rev. Lett. **90**, 132301 (2003).
- [9] D. K. Srivastava, J. Phys. G **35**, 104026 (2008).
- [10] S. Turbide, C. Gale, S. Jeon and G. Moore, Phys. Rev. C **72**, 014906 (2005).
- [11] J. Adams *et al.*, Phys. Rev. Lett. **97**, 162301 (2006); A. M. Hamed, J. Phys. G **35**, 104120 (2008); arXiv:0809.1462.
- [12] J. Frantz [PHENIX Collaboration], arXiv:0901.1393.